INTERNATIONAL JOURNAL OF QUANTUM CHEMISTRY SYMP. NO. 9, 569–578 (1975)

Large Electron–Phonon Interaction but Low-Temperature Superconductivity in LaB_6

A. J. ARKO, G. CRABTREE, J. B. KETTERSON, F. M. MUELLER, P. F. WALCH, AND L. R. WINDMILLER
Argonne National Laboratory, Argonne, Illinois 60439

AND

Z. FISK, R. F. HOYT, A. C. MOTA, AND R. VISWANATHAN
University of California at San Diego, La Jolla, California 92037

AND

D. E. ELLIS, A. J. FREEMAN, AND J. RATH
Northwestern University, Evanston, Illinois 60201

Abstract

Combined experimental and theoretical studies are reported of the Fermi surface, band structure, generalized magnetic susceptibility, electron-phonon enhancement factor λ, and superconducting transition temperature T_c of LaB_6. Whereas the unusually large λ values, ranging from 1.0 to 2.5, are expected to result in high T_c values, T_c is observed to be only 0.122°K. These results further emphasize the need for appropriate theoretical formulations for these systems.

1. Introduction

The strong covalent bonding in crystalline phases of boron compounds, which is responsible for their being extremely hard, refracting, and stable materials, also makes these compounds attractive as possible high-temperature superconductors. The hexaborides RB_6, which form interpenetrating simple cubic structures of cages of boron surrounding metalloid ions [1], are among the crystallographically simplest of the boride systems. We have studied in detail, both experimentally and theoretically, the electronic band structure, Fermi surface, generalized magnetic susceptibility $\chi(\boldsymbol{q})$, electron–phonon enhancement factor λ, and superconducting transition temperature T_c of high-purity single crystals of LaB_6. Surprisingly, although we deduce a very large λ (1.0 to 2.5) and hence expect that T_c would be large (naively, the use of the McMillan equation results in T_c ranging from 27 to 61°K), inductive measurements reveal $T_c = 0.122$°K. This striking failure of theory is related to the very different phonon spectra—"hard" boron-based modes and "soft" lathanum-based modes in LaB_6—compared with those of Nb used in the derivation of the McMillan equation.

2. The de Haas–van Alphen Effect

The single crystals used in these experiments were grown in an Al flux [2]. After solidification, the flux was dissolved with concentrated NaOH solution, leaving small, faceted, purple clusters. These were separated into individual grains by treatment with HNO_3. Magnetoresistivity showed that the total Fermi surface was open (connected) in the [110] and [001] directions. The single crystal sample used in the de Haas–van Alphen experiment weighed 200 micrograms and had a resistivity ratio of about 200. The de Haas–van Alphen measurements [3] were taken in fields up to 72 kG and temperatures down to 0.3°K. The resulting cross-sectional frequencies (areas) are plotted in Figure 1. The strongest de Haas–van Alphen oscillations were the nearly flat set (constant cross-sectional area) associated with the orbits marked X_1 in the (110) plane and X_2 in the (001) planes, respectively. Assuming a completely spherical shape, the cross-sectional area of 0.216 a.u.^{2} (at [100]) suggested a radius of 0.26 a.u., a volume of 0.074 a.u.^{3}, or that each sphere enclosed about 29 % of an electron (volume of BZ = 0.51 a.u.^{3}). Since the other areas of this sheet are bigger, this suggested that the "sphere" enclosed exactly 1/3 of an electron, that is, that there were three spheres centered at X_1 (or possibly at M, which has the same point group degeneracy as X).

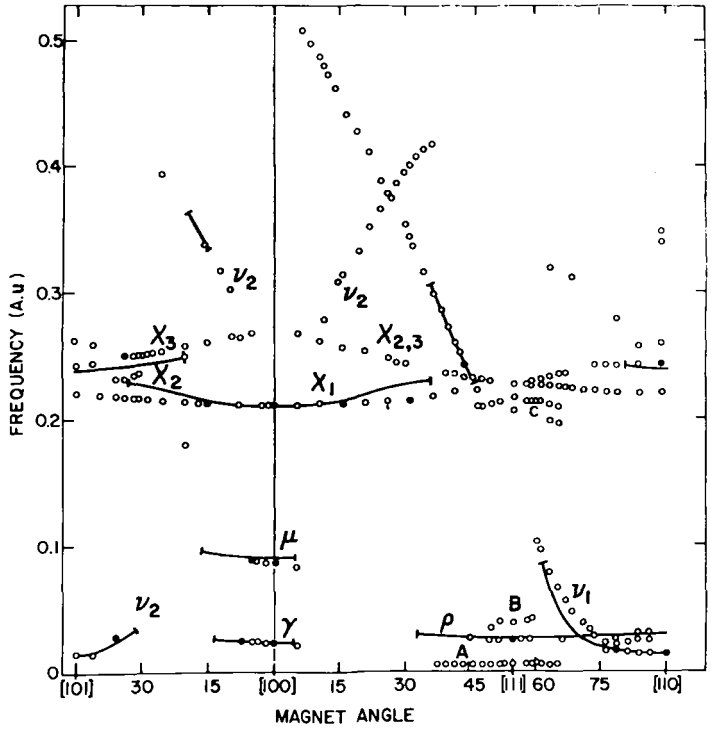

Figure 1. Extremal cross-sectional frequencies (areas) of the Fermi surface of LaB_6. The solid line is derived from an 11-term Fourier series model, fitted at the 15 solid dots.

We arbitrarily chose an X centered position connected by spherical necks in the [110] directions as our experimental model. This produced two [100] hole orbits centered at $\Gamma(\gamma)$ and $M(\mu)$, respectively, a threefold rosette ρ, and the important ν_1 orbits, centered at the [110] neck. The 15 points marked as the solid dots were used to fit an 11-term Fourier-based series, which included full-cubic symmetry [4]. The starting coefficients, derived from the band structure (discussed below), were sequentially varied until no further improvement was found. The final error, fitting to the areas given by the dots, was 0.0043 a.u.^{2}. The interpolated areas, based on this model, are given as the solid lines in Figure 1. This Fermi surface is shown as Figure 2 and may be understood as face-centered cubic stacks of connected spheres, similar to the Fermi surface of Cu.

3. Electronic Band Structure, Density of States, and Generalized Susceptibility

The electronic band structure was calculated by means of the discrete variational method (DMV), a method able to treat general nonspherical, nonmuffin-tin potentials [5], found to be important in systems like LaB_6.

The Hartree-Fock-Slater (HFS) effective Hamiltonian was

$$H = T + T_c + V_x \tag{1}$$

where the first two terms were the kinetic energy and Coulomb potential, respectively, and the exchange operator V_x was approximated by the local potential (in Hartree

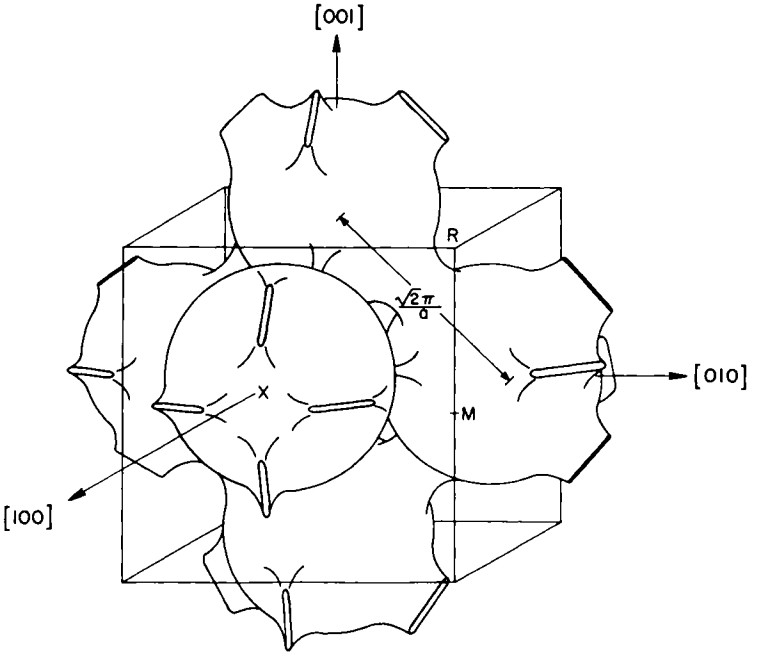

Figure 2. Fermi surface of LaB_6.

atomic units),

$$V_x = -3\alpha \left(\frac{3\rho}{8\pi} \right)^{1/3} \tag{2}$$

While various theoretical prescriptions for selection of a value for the adjustable parameter α have been presented in the literature [6–9], the current calculations were performed with the value of $\alpha = 1$ first suggested by Slater [6]. The crystal charge density ρ was approximated by the superposition of atomic (ionic) densities as

$$\rho = \sum_v \rho_v \tag{3}$$

It is important to note that the full crystal potentials are determined without making the usual muffin-tin averaging approximations. Thus all aspherical "crystal field" terms are retained. When the potential is approximated by its muffin-tin average, the solution to the Schrödinger equation is separable within each sphere, and the first principals APW and KKR methods can be applied [10]. This model of the potential, while adequate for most metals, is often a serious oversimplification when one is treating nonmetals and compounds [11–13].

Approximate eigenvalues and eigenfunctions of the HFS Hamiltonian are generated by means of a DMV which has been previously applied to a number of energy band problems [11, 12]. These calculations involve the selection of a discrete set of sample points in coordinate space, definition of an error functional connected with the Schrödinger equation, and minimization of the error functional over the discrete grid of sample points by a variational procedure. These direct numerical-variational techniques have been used with considerable success in treating potentials of very general form. A brief summary of the DMV follows; explanations in greater detail may be found elsewhere [13, 14].

The approximate wave functions are expanded in a fixed basis set,

$$\psi_i(\boldsymbol{k}, \boldsymbol{r}) = \sum_j \chi_j(\boldsymbol{k}, \boldsymbol{r})\, C_{ji}(\boldsymbol{k}) \tag{4}$$

where the basis functions $\chi_j(\boldsymbol{k}, \boldsymbol{r})$ are Bloch orbitals of wave vector $\boldsymbol{k}$ belonging to the jth irreducible representation of the crystal translation group. For this paper the basis orbitals are in turn constructed from linear combinations of Slater-type orbitals (STO) centered at nuclear sites. This LCAO basis is most appropriate for forming crystal wave functions for those systems in which the atomic character of the constituent atoms is maintained to a large degree. Systems in which the bonding between atoms is strong and highly directional are conveniently described in terms of this basis.

We define the error functional for state i at point $\boldsymbol{r}$ as

$$\delta_i(\boldsymbol{r}) = (H - \varepsilon_i)\, \psi_i(\boldsymbol{r}) \tag{5}$$

and minimize the expectation values $\langle \chi_j | \delta_i \rangle$ over some grid of sample points $\{\boldsymbol{r}_p\}$, obtaining the matrix secular equation

$$HC = SCE \tag{6}$$

for determining the variational coefficients $C_{ij}(\boldsymbol{k})$. These equations are identical to the conventional Rayleigh-Ritz equations, except that the matrix elements are given as a sample mean, such as

$$H_{ij} = \sum_p w(\boldsymbol{r}_p)\, \chi_i^*(\boldsymbol{r}_p)\, H\chi_j(\boldsymbol{r}_p) \tag{7}$$

Here $w(\boldsymbol{r})$ is a weight function, generally chosen so that matrix elements converge to their integral values as the number of sample points is increased. Careful choices of weight function and sample point distribution lead to rapid convergence to the Rayleigh–Ritz eigenvalues.

Basis functions for the variational calculations were constructed as Bloch sums of STO functions centered on the lanthanum and boron sites. Considerable experimentation was done by varying the number and type of STOs to determine the effects of basis truncation on the band energies. The bands discussed here were generated from a 134 STO function set as this represents a reasonable compromise between accuracy and computational cost. There are ten boron basis functions of roughly "double zeta" [15] quality on each ligand site. The lanthanum basis includes seven sets of d orbitals, but no f orbitals. After considerable testing, f-orbital contribution to energies near the Fermi surface was deemed to be inconsequential in comparison to lanthanum d-orbital and ligand orbital contributions. Convergence of band energies as a function of the number of sampling points per cell was also investigated. An optimum choice to achieve sufficient accuracy at reasonable cost was a 3972-point mesh. The metal sphere radius was compressed in order that the resulting high density of points would lead to an adequate description of the complicated wave function behavior near the lanthanum nucleus. The large number of interatomic sampling points made it possible to adequately converge the diffuse $5d$ and $6s$ lanthanum orbital contribution to the Bloch functions.

The energy bands for LaB_6 are plotted along symmetry lines in Figure 3; the corresponding Hamiltonian was generated from neutral atom configurations, with an exchange scaling parameter $\alpha = 1.0$. Aspherical (nonmuffin-tin) contributions to the crystal potential were found to be sizable. The input charge densities and atomic Coulomb potentials were computed from the accurate Hartree-Fock orbitals of Clementi [15]. Past experience indicates that the computed energy bands are relatively insensitive to the ionicity of the input atomic configurations [12]. The calculated energies are estimated to be converged to within ± 0.01 Ry. As expected, the bands show LaB_6 to have metallic properties with the Fermi energy lying inside the fourth band at -0.720 Ry.

The energy bands were calculated at 18 k points. This number was judged to be suitable for an adequate understanding of the Fermi surface and the density of states. Computer time per k point on the IBM-360/195 at Argonne National Laboratory was about 1000 seconds of CPU time with approximately 10,000 kbyte/sec of core charge. Fifteen of the k points were chosen to lie along high symmetry dirrections and three were points of lowest symmetry. An approximate balance of k-space volume per point was achieved by spreading the points on or near the $k = 0$, $\pi/4a$, $\pi/2a$, $3\pi/4a$, π/a planes in numbers roughly proportional to the planar area. Because of

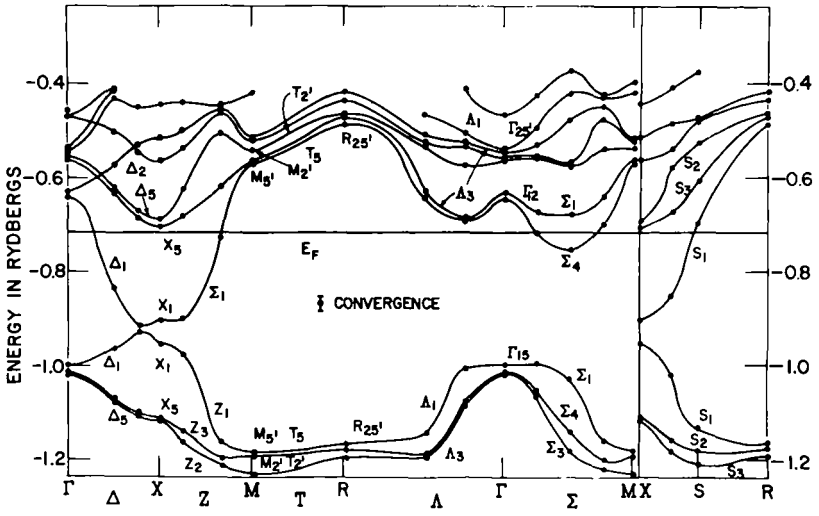

Figure 3. Electronic band structure of LaB_6 in the vicinity of E_F.

extreme complexity and length of these calculations, it was not feasible to fully test the sensitivity of the energy bands to scaling of the α parameter. However, the relevant eigenvalues at $k = 0$ (Γ point) were found to undergo an approximately rigid shift of $\sim +0.4$ Rydberg when α was varied from 1.0 to 2/3, the value suggested by Kohn, Sham and Gaspar [7, 8]. It is reasonable to assume that the shifting of the bands at other k points could also be roughly approximated by a rigid shift.

The band structure (Figure 3) shows an X centered sphere whose diameter (directly from the figure) is 3.77 cm or a radius of 0.28 a.u. The neck lies along the Γ to M direction, and has a diameter of 1.79 cm or a diameter of 0.27 a.u. compared to a model diameter of 0.25 a.u. The X to R radius is 1.60 cm or 0.24 a.u. compared to the Fermi surface model of 0.24 a.u. Again, due to cost, a nonrelativistic model was used. A few additional points were found on the symmetry axes used to plot Figure 3, since the details of the crossing near X and at the neck near $\sum_4$ helped us to understand the topology and absolute radii in the band model.

This set of 18 points was then fit to an interpolation scheme, here a symmetrized Fourier series. The 11-term fit was used (for each of the bands in Figure 3) to produce the density of states shown in Figure 4, and the Fermi energy of -0.72 Ry was found by direct integration. This set of Fourier coefficients was used to calculate a selected area from Figure 1. The error directly from the band structure was 0.013 a.u.^{2}, or about 6%.

Since no f basis functions were included in the calculations given in Figure 2, the wave functions at the Fermi energy are, within this model, a mixture of La 5*d* and B 2*s*–2*p* orbitals. (In preliminary calculations we found [16] that the energy eigenvalues near the Fermi energy were insensitive to the presence or absence of f states in the basis.) We interpret the two sets of bands near -1.2 and -0.6 Ry as due to bonding and antibonding 2*s*–2*p* boron orbitals (as in the model calculations [17] of Longuet-Higgens and de V. Roberts) combined with structure from the La 5*d* bands.

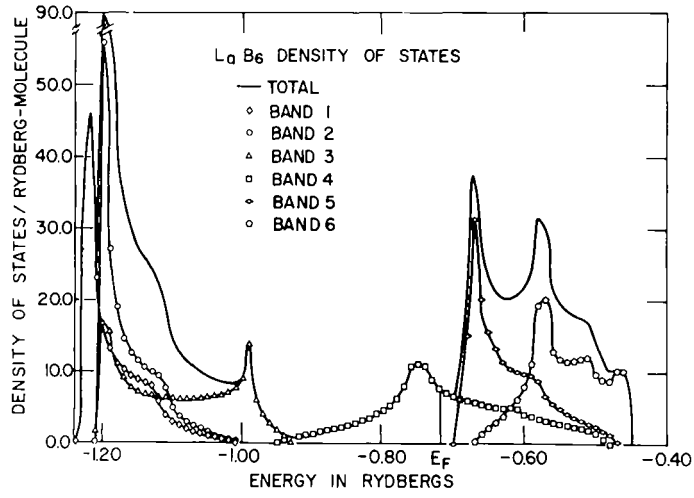

Figure 4. Electronic density of states of LaB_6 in the vicinity of E_F.

As discussed by Freeman and coworkers elsewhere in this volume [18], divergences in the generalized static electronic susceptibility determines possible instabilities in metals. For systems like LaB_6, our interest lies in the fact that peaks in $\chi^0(q)$ may lead to "soft" phonon modes which would strongly affect the superconducting properties.

We have calculated the momentum dependence of the RPA susceptibility of the 44th band, using an 11-term Fourier series fit to the band structure and the analytic tetrahedron linear energy method of Rath and Freeman [19]. The results are shown in Figure 5. Note that the ordinate has been scaled in each of the three directions so that they coincide at 1/2 of a respective reciprocal lattice distance.

The calculated $\chi^0(q)$ shows a large maximum approximately two times the value of χ^0 ($q = 0$) at the zone boundary for q along the [111] direction and a smaller maximum for q along the [110] direction. Although we have not included the effects of matrix elements, we believe that (in a simple approximation) the weak momentum dependence of the $5d$ La wave function would not greatly reduce $\chi^0(q)$ near the dominant [111] peak. The existence of this peak suggests two important conclusions for further experimental observations, (1) in systems like LaB_6 which are not magnetic, the peak leads to "soft" phonon modes and large electron–phonon coupling; (2) in rare-earth systems with f electrons the peak leads to a simple rock-salt commensurate antiferromagnetic ordering. Both effects should be visible through neutron scattering on compounds made from isotopically pure boron 11.

4. Electron–Phonon Interaction and Superconductivity

In Table I we have abstracted measured and calculated masses together with deduced enhancements [20]. If we assume that these enhancements are entirely due to the electron–phonon interaction, then the coupling is very large. (Indeed one must immediately speculate why LaB_6 does not undergo a phase transition. We believe

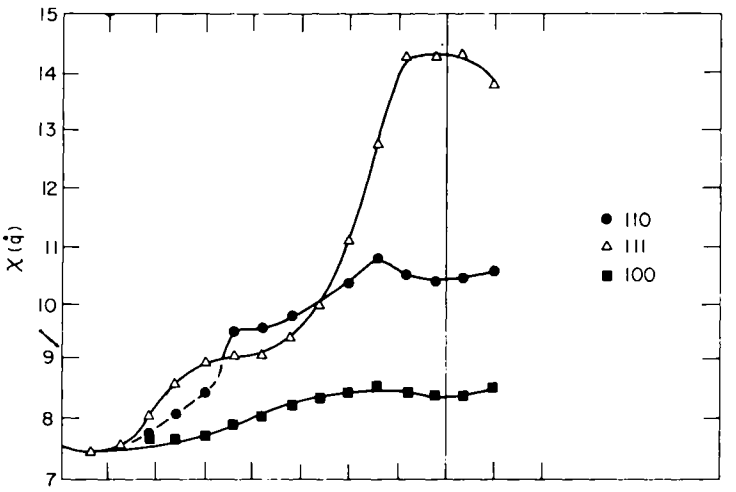

Figure 5. RPA susceptibility in the [100], [110], and [111] directions of LaB_6.

that the answer lies in the rigidity of the covalently bonded boron cage.) Of interest, too, is that the optical mass [21] is about the same as the band mass. Since the bands in the vicinity of the Fermi surface are nearly isotropic (we ignore the small necks), the (unenhanced) density states mass and optical mass as defined by Cohen [22] should be the same. Due to the frequency dependence of the electron–phonon interaction, the optical mass appears "undressed." The comparison of the optical mass with the (enhanced) specific heat mass provides a "band-structureless" estimate of the electron-phonon coupling, a fact which has not been emphasized enough before [23].

Finally we consider the superconductivity of LaB_6. Chemically, Y and La behave similarly in many compounds. Elemental La, in its dhcp phase, has a T_c of 4.9°K, where Y is superconducting only under high pressure. YB_6 is a superconductor with a transition temperature [24] T_c of about 7°K. Yet from studies [24] of a series of

TABLE I. Electronic masses and enhancements in LaB_6.

γ	Electronic specific heat[a]	4.75 mJ/K^2	2.01 states/eV
N(0)	Density of States at E_F	7.70 states/Ry	0.57 states/eV
	$\lambda_1 = [\gamma/N(0)] - 1 = 2.53$		
m_{op}	optical mass[b]	0.21-0.33	electron masses
m_t	band orbital mass on ball normal to [100]	0.29	electron masses
m_{cy}	experimental mass on ball normal to [100]	0.62	electron masses
	$\lambda_2 = (m_{cy}/m_t) - 1 = 1.14$		

[a]Reference [20].
[b]Reference [21].

$La_xY_{1-x}B_6$ alloys, superconductivity is rapidly suppressed at about 70% La. Direct measurement on samples grown from extremely pure La (0.999999) and B (0.999999) showed an inductive superconducting transition temperature of 0.122°K. Samples grown from less pure materials had lower or broader transition temperatures. A magnetic field of a few gauss quenched superconductivity: in spite of the "good" metallic conductivity, the susceptibility was then slightly diamagnetic, $(-)5.0 \pm 0.5 \times 10^{-7}$ EMU/g (or in density of states units, $(-)0.015$ states/eV) compared to a Pauli susceptibility based on the band density of states of $(+)1.84 \times 10^{-5}$ EMU/g.

By contrast, if we use our highest λ, an average specific heat Debye temperature [20] of 438°K, and an average transition metal Coulomb pseudopotential [15] μ^* of 0.13 in the McMillan [25] equation, we arrive at a T_c of 61°K; using the smaller λ, the result is 27°K. (Based on these parameters, LaB_6 is very reminiscent of another low-density-of-states high-lambda material, NbN, whose T_c is about 15°K.)

But as stated, LaB_6 is a superconductor only at very low temperatures. We believe that the explanation is that the phonon sprectum of LaB_6 has "hard" boron-based modes and "soft" lanthanum-based modes, and is rather different from the Nb phononic structure used in the deviation of the McMillan equation. Thus it appears that the Eliashberg equations need to be reexamined in detail for each new class of material before a reliable McMillan-type equation can accurately predict T_c.

Acknowledgment

This work was supported by the U.S. Energy Research and Development Administration, the National Science Foundation, the Air Force Office of Research, and the Advanced Research Projects Agency.

Bibliography

[1] L. Pauling, *The Nature of the Chemical Bond* (Cornell University Press, Ithaca, N.Y., 1960); E. L. Muetterties, Ed., *The Chemistry of Boron and Its Compounds* (Wiley, New York, 1967); H. J. Goldschmidt, *Interstitial Alloys* (Butterworth, London, 1967), ch. 6.
[2] Z. Fisk, A. S. Copper, P. H. Schmidt, and R. N. Castellano, Mat. Res. Bull. 7, 285 (1972).
[3] L. R. Windmiller and J. B. Ketterson, Rev. Sci. Inst. **39**, 1672 (1968).
[4] J. B. Ketterson, F. M. Mueller, and L. R. Windmiller, Phys. Rev. **186**, 656 (1969).
[5] D. E. Ellis and G. S. Painter, in *Computational Methods in Band Theory*, P. M. Marcus, J. F. Janak, and A. R. Williams, Eds. (Plenum Press, New York, 1971).
[6] J. C. Slater, Phys. Rev. **81**, 385 (1951).
[7] W. Kohn and L. J. Sham, Phys. Rev. **140**, A1133 (1965).
[8] R. Gaspar, Acta Phys. Acad. Sci. Hung. **3**, 263 (1954).
[9] I. Lindgren, Ark. Fys. **31**, 59 (1965); Phys. Lett. **19**, 382 (1965).
[10] *Methods in Computational Physics*, vol. 8, B. Adler, S. Fernbach, and M. Rotenberg, Eds. (Academic Press, New York, 1968).
[11] G. S. Painter and D. E. Ellis, Phys. Rev. **B1**, 4747 (1970); D. E. Ellis and G. S. Painter, Phys. Rev. **B2**, 2887 (1970).
[12] P. F. Walch and D. E. Ellis, Phys. Rev. **B8**, 5920 (1973).
[13] D. E. Ellis and G. S. Painter, in *Computational Methods in Band Theory*, P. M. Marcus, J. F. Janak, and A. R. Williams, Eds. (Plenum Press, New York, 1971), p. 271; G. S. Painter and D. E. Ellis, *ibid*, p. 276.
[14] D. E. Ellis, Int. J. Quant. Chem. **S2**, 35 (1968); G. S. Painter and D. E. Ellis, Int. J. Quant. Chem. IIIS, 801 (1970).

[15] E. Clementi, IBM J. Res. Dev. Suppl. **9**, 2 (1965).
[16] P. F. Walch, D. E. Ellis, and F. M. Mueller (in preparation).
[17] H. C. Longuet-Higgins and M. de V. Roberts, Proc. Roy. Soc. (London) **230A**, 336 (1954).
[18] A. J. Freeman, H. W. Myron, J. Rath, R. P. Gupta, Int. J. Quant. Chem. **S9**, 535 (1975).
[19] J. Rath, and A. J. Freeman, Phys. Rev. **B 15**, 2109 (1975).
[20] R. S. Viswanathan (private communication).
[21] E. Kierzek-Pecold, Phys. Stat. Sol. **33**, 523 (1969).
[22] M. H. Cohen, Phil. Mag. **3**, 762 (1958).
[23] See the discussion by E. Stern, in *Optical Properties and Electronic Structure of Metals and Alloys*, F. Abeles, Ed. (North-Holland Publ., Amsterdam, 1966), p. 33, and the remarks of others at the conference.
[24] Z. Fisk (private communication, to be published).
[25] W. L. McMillan, Phys. Rev. **167**, 331 (1967), and references therein.

Received March 10, 1975.